
FIT: a Fast and Accurate Framework for Solving Medical Inquiring and Diagnosing Tasks

Weijie He*

Department of Computer Science &
Institute of Artificial Intelligence & BRNist
Tsinghua University
hwj19@mails.tsinghua.edu.cn

Xiaohao Mao*

Department of Computer Science &
Institute of Artificial Intelligence & BRNist
Tsinghua University
mxh19@mails.tsinghua.edu.cn

Chao Ma

Department of Engineering
University of Cambridge
cm905@cam.ac.uk

Yu Huang

Tencent Jarvis Lab
yorkeyhuang@tencent.com

José Miguel Hernández-Lobato

Department of Engineering
University of Cambridge
jmh233@cam.ac.uk

Ting Chen

Department of Computer Science &
Institute of Artificial Intelligence & BRNist
Tsinghua University
tingchen@tsinghua.edu.cn

Abstract

Automatic self-diagnosis provides low-cost and accessible healthcare via an agent that queries the patient and makes predictions about possible diseases. From a machine learning perspective, symptom-based self-diagnosis can be viewed as a sequential feature selection and classification problem. Reinforcement learning methods have shown good performance in this task but often suffer from large search spaces and costly training. To address these problems, we propose a competitive bipartite framework, called FIT, which uses an information-theoretic reward to determine what data to collect next. FIT improves over previous information-based approaches by using a multimodal variational autoencoder (MVAE) model and a two-step sampling strategy for disease prediction. Furthermore, we propose novel methods to substantially reduce the computational cost of FIT to a level that is acceptable for practical online self-diagnosis. Our results in two simulated datasets show that FIT can effectively deal with large search space problems, outperforming existing RL baselines. Moreover, using several public medical datasets, we show that FIT is a competitive alternative in various real-world settings.

1 Introduction

In healthcare, as a reference when patients selecting departments for hospital visits, self-diagnosis through online services is a promising approach for reducing costs and still maintaining wide accessibility. With the explosive development of the mobile internet, the feasibility and potential of access to online self-diagnosis in the healthcare domain have increased. A growing number of adults first attempt to self-diagnose their diseases through online search services instead of walking into a hospital. According to a 2012 survey [29], 35% of U.S. adults regularly use the internet

*Equal contribution.

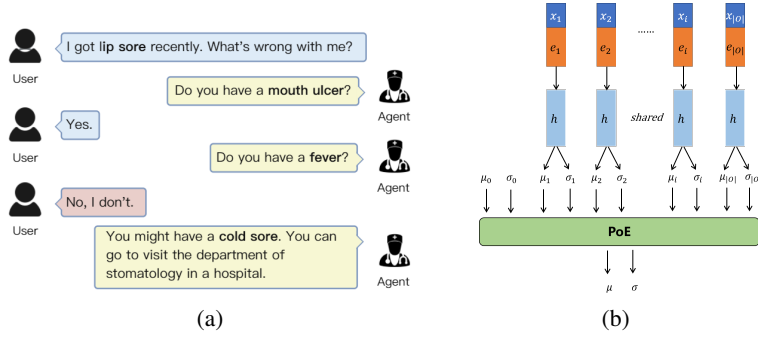


Figure 1: (a) A demonstration of the online self-diagnosis process. (b) Overview of Products-of-Experts (PoE) encoder.

to self-diagnose. However, existing online search-based services for self-diagnosis often return irrelevant information and sometimes absurd results.

As described by Ledley and Lusted [19], a disease diagnosis process includes three sequential steps: (i) a patient presents an initial symptom, (ii) a doctor inquires a patient with a series of reasonable questions, (iii) a final diagnosis for a disease is given by the doctor. In the case of online self-diagnosis, the above process is referred to as a *symptom checking* task, and it is an agent who implements inquiry and diagnosis instead of the doctor. Figure 1(a) presents an example of online self-diagnosis.

It is noteworthy that most previous deep learning methods, like DoctorAI [4], RETAIN [5] and Dipole [23], model sequential electronic health record data by examining historical visits, and predict future disease risk of patients, which differs from our work. All of them are unable to deal with *cold-start* users [32], i.e., users do not have historical records of hospital visits. Unfortunately, online self-diagnosis has little prior information about individuals than those in public datasets, e.g., MIMIC-III. The system should continue questioning and answering with users to make an accurate and confident diagnosis.

From the healthcare perspective, disease-prediction accuracy is the primary aim of symptom checking. High accuracy requires a long list of possible symptoms, e.g., most existing questionnaire systems acquire a large number of symptom values from patients through exhaustive questions [30, 20]. It is inefficient and time-consuming for both patients and experts. Therefore, the other design goal of symptom checking is efficiency, i.e., the number of inquiries should be as low as possible.

From the machine learning perspective, symptom checking can be viewed as a sequential cost-sensitive feature selection and classification problem. Reinforcement learning (RL) methods have shown good performance in this task [31, 12, 13, 28, 35]. However, they often suffer from large search spaces and struggle during training. EDDI [22], a framework for instance-based active feature acquisition, gives an alternative solution, which chooses the next feature to observe by maximizing a defined information reward over all features. EDDI uses a Partial VAE to handle data with missing values. Such a model can deal with the situation where an agent just knows part of the information from patients while inquiring. Although promising, the EDDI framework is limited by its high computational cost when the number of symptoms is very high.

We propose FIT, a competitive bipartite framework to automate inquiring and diagnosing tasks based on EDDI to address these problems. The contributions of this paper are:

A novel non-RL framework for inquiring and diagnosing tasks. FIT is more practical and suitable for *real-life diagnosis* since it can **handle huge feature spaces with low time cost and show great universality among diverse settings**, while RL baselines typically struggle in those settings.

New experimental settings and diverse evaluations. We initiate the evaluation on colossal feature spaces based on rare disease datasets and first propose to verify the effectiveness of simulated train data on public knowledge bases. Most previous literature validated their method on either simulated or real-world datasets, while in our experiments, FIT outperforms several SOTA RL methods on both datasets, including a diabetes dataset that symptom-checking RL baselines could not handle.

Improvements on model. We propose a self-attention diagnosis model and use a multi-modal variational autoencoder (MVAE) [34] as a probabilistic model dealing with partially observed data. We also adopt a two-step sampling strategy for EDDI [22]. All these improve the diagnostic accuracy.

Significant speedup of computations for symptom checking. We accelerate the inquiry steps so that they take less than one second on average, making our framework practical in real-life settings. At any inquiry step, we first ignore irrelevant symptoms that are unlikely to co-occur with the ones currently observed, and second, when computing the information reward, we propose an efficient approximation strategy. Both modifications can reduce the time cost of our framework substantially without degrading prediction accuracy.

2 Background

In this paper, we formulate symptom checking as the feature acquisition problem. Let S denote the set of all possible symptoms, and ϕ denote the set of possible diseases. Suppose \mathbf{x}_i denotes the presence of symptom $i \in S$, that is $\mathbf{x}_i = 1$ if symptom i is present, and $\mathbf{x}_i = 0$ otherwise. Similarly, \mathbf{x}_ϕ are the one-hot categorical variables that indicate which disease is present. Then, we are interested in predicting the target variables \mathbf{x}_ϕ given corresponding observed features \mathbf{x}_O ($\mathbf{x}_\phi \cap \mathbf{x}_O = \emptyset$), where $O \subset S$ is the subset of symptom status that are currently observed, and $U = S \setminus O$ are the unobserved ones. More specifically, we consider which symptom $\mathbf{x}_i \in \mathbf{x}_U$ to inquire next so that our belief regarding \mathbf{x}_ϕ can be optimally improved.

2.1 EDDI Framework Formulation

A variational autoencoder (VAE) [14] defines a generative model of the form $p(\mathbf{x}, \mathbf{z}) = \prod_j p_\theta(\mathbf{x}_j | \mathbf{z}) p(\mathbf{z})$ in which the data \mathbf{x} is generated from latent variables \mathbf{z} , $p(\mathbf{z})$ is a prior, e.g., spherical Gaussian. $p_\theta(\mathbf{x} | \mathbf{z})$ is given by a neural network decoder with parameters θ , which specify a simple likelihood, e.g., Bernoulli. A VAE uses another neural network with parameters Φ as an encoder to produce a variational approximation of the posterior, that is, $q_\Phi(\mathbf{z} | \mathbf{x})$. A VAE is trained by maximizing an evidence lower bound (ELBO):

$$\mathbf{E}_{q_\Phi(\mathbf{z} | \mathbf{x})} [\log p_\theta(\mathbf{x} | \mathbf{z})] - \beta \cdot D_{\text{KL}}[q_\Phi(\mathbf{z} | \mathbf{x}) \| p(\mathbf{z})], \quad (1)$$

where β is the weight to balance the two terms in the expression. The ELBO is usually optimized by stochastic gradient descent using the reparameterization trick [14].

EDDI is a recently proposed solution [22] that is designed to solve the formulated feature acquisition problem efficiently using a VAE. EDDI chooses the next feature \mathbf{x}_i to observe by maximizing over i the information reward

$$R(i, \mathbf{x}_O) = \mathbf{E}_{\mathbf{x}_i \sim p(\mathbf{x}_i | \mathbf{x}_O)} D_{\text{KL}} [p(\mathbf{x}_\phi | \mathbf{x}_i, \mathbf{x}_O) \| p(\mathbf{x}_\phi | \mathbf{x}_O)], \quad (2)$$

where D_{KL} is the Kullback-Leibler divergence between two distributions. The conditionals $p(\mathbf{x}_i | \mathbf{x}_O)$, $p(\mathbf{x}_\phi | \mathbf{x}_O, \mathbf{x}_i)$, and $p(\mathbf{x}_\phi | \mathbf{x}_O)$ are described by a VAE. Unfortunately, estimating the values of these quantities in Eqn. 2 is too expensive in practice. To avoid this problem, Ma et al. [22] show that Eqn. 2 can be estimated efficiently by using VAE encoding distributions:

$$\begin{aligned} \hat{R}(i, \mathbf{x}_O) &= \mathbf{E}_{\mathbf{x}_i \sim \hat{p}(\mathbf{x}_i | \mathbf{x}_O)} D_{\text{KL}} [q(\mathbf{z} | \mathbf{x}_i, \mathbf{x}_O) \| q(\mathbf{z} | \mathbf{x}_O)] - \\ &\mathbf{E}_{\mathbf{x}_\phi, \mathbf{x}_i \sim \hat{p}(\mathbf{x}_\phi, \mathbf{x}_i | \mathbf{x}_O)} D_{\text{KL}} [q(\mathbf{z} | \mathbf{x}_\phi, \mathbf{x}_i, \mathbf{x}_O) \| q(\mathbf{z} | \mathbf{x}_\phi, \mathbf{x}_O)], \end{aligned} \quad (3)$$

where $q(\cdot)$ is the encoder function of the underlying VAE model. The encoder is parameterized by a permutation invariant set function (detailed in the next section) so that it can produce a Gaussian approximation of the posterior of \mathbf{z} conditioned on any set of observed variables. The first term of Eqn. 3 quantifies how much information \mathbf{x}_i provides about \mathbf{z} , and the second term quantifies how much information \mathbf{x}_i provides about \mathbf{z} *in addition to* \mathbf{x}_ϕ . A feature \mathbf{x}_i will be penalized by the second term if it is informative about \mathbf{z} but not about \mathbf{x}_ϕ . All quantities in the KL divergences above can be computed analytically thanks to the Gaussian approximations. The expectations in Eqn. 3 can be approximated by Monte Carlo, averaging over samples $\hat{\mathbf{x}}_\phi, \hat{\mathbf{x}}_i \sim p(\mathbf{x}_\phi, \mathbf{x}_i | \mathbf{x}_O)$ that can be shared between the two terms in Eqn. 3. The number of samples is denoted as M .

3 Methodology

Our FIT framework consists of an inquiry branch and a diagnosis branch to achieve a more accurate and efficient process. In this section, we first present a prior conditional probability guided classifier as the diagnosis part of our framework, then introduce our improvements on the model and sampling scheme of the EDDI framework as the inquiry part. Next, we elaborate on how to accelerate computations in the case of symptom checking. Finally, we introduce the diagnostic bases and the stop criterion of the inquiry process. We present a summary of FIT **in the Appendix**.

3.1 Diagnosis Model

Note that we may want to make predictions for possible diseases at any step of the feature collection process. This is something that RL methods are **sub-optimal** at since they use a classifier that is trained to make predictions once the RL agent stops collecting data and not at any stages of the data collection process. FIT does not have this problem. In particular, we denote by $f_\phi(\cdot)$ the function returning the disease prediction distribution $p(\mathbf{x}_\phi|\mathbf{x}_O)$, which takes \mathbf{x}_S as input and \mathbf{x}_U are imputed.

Specifically, inspired by Choi et al. [6], we use a self-attention mechanism guided by \mathbf{M} and \mathbf{P} to learn the embedding vector \mathbf{e} of each variable in \mathbf{x}_S and \mathbf{x}_ϕ . \mathbf{M} has negative infinities where connections are not allowed, otherwise zeros. \mathbf{P} denotes the matrix of conditional probabilities between all variables based on co-occurrence. We list the details of settings of \mathbf{M} and \mathbf{P} in the Appendix. Defining $\mathbf{A}^{(j)}$ as the attention matrix and $\mathbf{E}^{(j)}$ as the embedding vectors of j -th block, the model $f_\phi(\cdot)$ of J self-attention blocks can be formulated as:

$$\mathbf{A}^{(j)} = \text{softmax}\left(\frac{\mathbf{Q}^{(j)}\mathbf{K}^{(j)\top}}{\sqrt{d}} + \mathbf{M}\right), \quad (4)$$

$\mathbf{E}^{(j)} = \text{MLP}^{(j)}(\mathbf{P}\mathbf{E}^{(j-1)}\mathbf{W}_V^{(j)})$ when $j = 1$, $\mathbf{E}^{(j)} = \text{MLP}^{(j)}(\mathbf{A}^{(j)}\mathbf{E}^{(j-1)}\mathbf{W}_V^{(j)})$ when $j > 1$, where $\mathbf{Q}^{(j)} = \mathbf{E}^{(j-1)}\mathbf{W}_Q^{(j)}$, $\mathbf{K}^{(j)} = \mathbf{E}^{(j-1)}\mathbf{W}_K^{(j)}$ and d is the column size of $\mathbf{W}_K^{(j)}$. $\mathbf{W}_Q^{(j)}$, $\mathbf{W}_K^{(j)}$ and $\mathbf{W}_V^{(j)}$ are trainable parameters. $\mathbf{E}^{(0)}$ is constructed by concatenation: if $i \in S$, $\mathbf{E}_i^{(0)} = [\mathbf{x}_i, \mathbf{e}_i]$; if $i \in \phi$, $\mathbf{E}_i^{(0)} = [0, \mathbf{e}_i]$. The prediction distribution is obtained from the last embedding vectors of \mathbf{x}_ϕ : $p(\mathbf{x}_\phi|\mathbf{x}_O) = \text{softmax}(\text{MLP}(\mathbf{E}_\phi^{(J)}))$. As a regularization term, $\sum_j L_{reg}^{(j)}$ is summed to the prediction loss term during training, where

$$L_{reg}^{(j)} = D_{\text{KL}}(\mathbf{P}||\mathbf{A}^{(j)}) \text{ when } j = 1, L_{reg}^{(j)} = D_{\text{KL}}(\mathbf{A}^{(j-1)}||\mathbf{A}^{(j)}) \text{ when } j > 1, \quad (5)$$

and \mathbf{P} serves as the guidance for deriving the attention $\mathbf{A}^{(j)}$. We train $f_\phi(\cdot)$ on complete data, i.e., $\mathbf{x}_O = \mathbf{x}_S$. The learned embeddings are used to train the inquiry model.

3.2 Inquiry Model

During active variable selection, the inference network of the VAE should be capable to handle arbitrary partial observations of feature variables. The EDDI framework [22] proposed a permutation invariant set function, given by

$$\mathbf{c}(\mathbf{x}_O) := g(h(\mathbf{s}_1), h(\mathbf{s}_2), \dots, h(\mathbf{s}_{|O|})), \quad (6)$$

where $|O|$ is the number of observed variables and \mathbf{s}_i is obtained from the product of the feature value \mathbf{x}_i and an embedding vector \mathbf{e}_i describing the i -th feature. The value of the embedding vector is optimized during training together with the recognition network. $h(\cdot)$ is a neural network and $g(\cdot)$ is summation or max-pooling operation.

3.2.1 Product of Experts (PoE) Encoder

Wu and Goodman [34] proposed the Multimodal Variational Autoencoder (MVAE) to capture a joint distribution across data modalities and flexibly support missing multimodal data. The MVAE assumes conditional independence among data modalities and uses a **PoE encoder** to approximate the joint posterior for the latent variables. The PoE approximate posterior, including a prior expert $p(\mathbf{z})$, is given by

$$q(\mathbf{z}|\mathbf{x}_1, \dots, \mathbf{x}_{|O|}) \propto p(\mathbf{z}) \prod_i q(\mathbf{z}|\mathbf{x}_i), \quad (7)$$

where $q(\mathbf{z}|\mathbf{x}_i)$ is an inference network denoting the expert with the i -th observed variable \mathbf{x}_i .

In our implementation of the PoE encoder, we first, construct \mathbf{s}_i by concatenation: $\mathbf{s}_i = [\mathbf{x}_i, \mathbf{e}_i]$. **Note that \mathbf{e}_i is trained by the diagnosis model and fixed during training.** Then we use an MLP with 4 hidden layers as $h(\cdot)$ to map the input \mathbf{s}_i to a factorized Gaussian distribution in latent space with mean vector $\boldsymbol{\mu}_i$ and marginal standard deviation $\boldsymbol{\sigma}_i$. Because a product of Gaussian experts is itself Gaussian [3], when $p(\mathbf{z})$ and $q(\mathbf{z}|\mathbf{x}_i)$ are Gaussian, we can compute the mean and covariance parameters for the distribution in Eqn. 7 easily:

$$\boldsymbol{\mu} = \left(\sum \boldsymbol{\mu}_i \mathbf{T}_i\right) \left(\sum \mathbf{V}_i^{-1}\right)^{-1}, \mathbf{V} = \left(\sum \mathbf{V}_i^{-1}\right)^{-1}, \quad (8)$$

where $\boldsymbol{\mu}$ and \mathbf{V} are the mean vector and covariance matrix, respectively. The structure of our PoE encoder is illustrated in Figure 1(b). The decoder, $p(\mathbf{x}|\mathbf{z})$, is given by a product of Bernoulli distributions whose probabilities are specified by a 4-layer MLP that receives as input \mathbf{z} .

Given a dataset with no missing variables, if we trained the PoE encoder on all the available data, its performance would then be deficient when the input presents missing entries since the PoE encoder never dealt with such a situation at training time. To address this, we follow Wu and Goodman [34] and drop a random fraction of the fully observed variables for each data point during training.

3.2.2 Two-step Sampling Strategy

To estimate the information reward, we approximate expectations by Monte Carlo. In particular, we average over samples $\hat{\mathbf{x}}_\phi, \hat{\mathbf{x}}_i \sim p(\mathbf{x}_\phi, \mathbf{x}_i|\mathbf{x}_O)$. This can be implemented by first sampling $\hat{\mathbf{z}} \sim q(\mathbf{z}|\mathbf{x}_i)$, and then $\hat{\mathbf{x}}_\phi, \hat{\mathbf{x}}_i \sim \hat{p}(\mathbf{x}_\phi, \mathbf{x}_i|\mathbf{z})$, where $\hat{p}(\mathbf{x}_\phi, \mathbf{x}_i|\mathbf{z})$ is the decoder network in the EDDI VAE. However, we propose a better sampling method for FIT, which samples $\hat{\mathbf{x}}_i$ and $\hat{\mathbf{x}}_\phi$ in two steps. Note that

$$p(\mathbf{x}_\phi, \mathbf{x}_i|\mathbf{x}_O) = p(\mathbf{x}_\phi|\mathbf{x}_i, \mathbf{x}_O) \cdot p(\mathbf{x}_i|\mathbf{x}_O). \quad (9)$$

Therefore, we propose to sample $\hat{\mathbf{x}}_i$ from the VAE by sampling $\hat{\mathbf{z}} \sim q(\mathbf{z}|\mathbf{x}_O)$, and then $\hat{\mathbf{x}}_i \sim \hat{p}(\mathbf{x}_i|\mathbf{z})$. Next we sample $\hat{\mathbf{x}}_\phi$ from $f_\phi(\cdot)$, of which the input is $\hat{\mathbf{x}}_i \cup \mathbf{x}_O$ and \mathbf{x}_U are imputed by zero. In this way, we are using two networks (the VAE decoder and $f_\phi(\cdot)$) to decompose the approximation of the joint posterior. By combining the generative model and the classification model, we can help improve the performance of the entire framework. An ablation study can be found in the Appendix.

3.3 Speedup for Symptom Checking

The computational cost of the EDDI framework [22] is $O(T \cdot N \cdot M)$, where T is the number of maximum inquiry steps, N is the number of total features, and M is the number of samples used to calculate Eqn. 3 in the Monte Carlo approximation. It is too high for an online symptom checking service, of which N can be hundreds or thousands. This section shows how we can reduce the cost by a large amount by taking advantage of feature sparsity.

3.3.1 Filtering Irrelevant Symptoms

At each step, the EDDI framework chooses variable \mathbf{x}_i from U to maximize the information reward. Under the setting of inquiry for symptoms, we can filter irrelevant symptoms to reduce the number of variables that need to be queried.

For every symptom i , we calculate the set S_i of additional symptoms which may appear together with symptom i in one patient with high probability, according to training data statistics. More specifically, a symptom $j \in S_i$ if $p_{data}(\mathbf{x}_j = 1|\mathbf{x}_i = 1)$ is larger than a given threshold p . We set p to 0 in experiments. The set of candidate symptoms is initialized to S_i when symptom i is present at the beginning of the inquiry. Every time the framework selects an additional positive symptom j , we update the candidate symptoms to be the intersection of the current set and S_j .

3.3.2 Approximation of the Reward

The reward $\hat{R}(i, \mathbf{x}_O)$ in Eqn. 3 is approximated by averaging over M samples $\hat{\mathbf{x}}_\phi, \hat{\mathbf{x}}_i \sim p(\mathbf{x}_\phi, \mathbf{x}_i|\mathbf{x}_O)$. Note that \mathbf{x}_i is binary and \mathbf{x}_ϕ is discrete among $|\phi|$ diseases in symptom checking. Indeed we just need compute rewards of $2 \cdot |\phi|$ different combinations of \mathbf{x}_i and \mathbf{x}_ϕ , and figuring up a weighted average by $p(\mathbf{x}_\phi, \mathbf{x}_i|\mathbf{x}_O)$ that is solved by the two-step sampling strategy in Sec. 3.2.2. Then the time cost is $O(T \cdot N \cdot (2|\phi|))$. In what follows we show how to speed up it by reducing $2|\phi|$.

Table 1: Performance of REFUEL [28] and FIT on the simulated rare disease dataset based on HPO. The results of FIT are shown in percentage with a 95% confidence interval with 5 random runs.

#DISEASES	REFUEL [28]				FIT			
	TOP1	TOP3	TOP5	#STEPS	TOP1	TOP3	TOP5	#STEPS
500	64.33	73.14	75.34	8.09	76.23 ± 0.47	84.17 ± 0.53	86.99 ± 0.41	5.34 ± 0.04
1000	40.08	62.67	67.42	14.19	68.65 ± 0.29	77.23 ± 0.45	80.35 ± 0.47	11.09 ± 0.08

Table 2: Performance of REFUEL [28] and FIT on the simulated SymCAT dataset. The results of FIT framework are shown in percentage with a 95% confidence interval with 5 random runs.

#DISEASES	REFUEL [28]				FIT			
	TOP1	TOP3	TOP5	#STEPS	TOP1	TOP3	TOP5	#STEPS
200	53.76	73.12	79.53	8.24	55.65 ± 0.25	80.71 ± 0.26	89.32 ± 0.29	12.02 ± 0.06
300	47.65	66.22	71.79	8.39	48.23 ± 0.25	73.82 ± 0.32	84.21 ± 0.17	13.10 ± 0.05
400	43.01	59.65	68.89	8.92	44.63 ± 0.29	69.22 ± 0.11	79.54 ± 0.15	14.42 ± 0.03

For one thing, the number of symptoms that a patient of a specific disease suffers from is much smaller than the number of possible symptoms for the disease. With such a sparse feature space, the inquiry process should acquire positive symptoms; otherwise, there is not enough evidence for the diagnosis component to perform accurate predictions [28]. Motivated by this, we encourage FIT to discover positive symptoms by discarding combinations of \mathbf{x}_i and \mathbf{x}_ϕ when $\hat{\mathbf{x}}_i = 0$, i.e., set their rewards to 0. Hence the number of computed combinations of \mathbf{x}_i and \mathbf{x}_ϕ is reduced by half.

For another, with a large $|\phi|$, almost every $f_\phi(\cdot)$ is long-tailed. We sort all different values of \mathbf{x}_ϕ by its probability in $f_\phi(\cdot)$, calculated by the two-step sampling strategy in Sec. 3.2.2, and discard ones beyond the top 90 percent of total probabilities or less than $1/|\phi|$. The average number of computed combinations can be further controlled in single figures experimentally.

We present several studies in the Appendix to show that these techniques result in a speedup of **70x**, from 32.52 seconds per step to 0.45, without degrading accuracy.

3.4 Diagnostic Bases and Stop Criterion

As said in Sec. 3.1, $f_\phi(\cdot)$ is trained with no missing variables. To make predictions in every step, we impute the missing variables \mathbf{x}_U of input by drawing M samples from $\hat{\mathbf{x}}_U \sim p(\mathbf{x}_U|\mathbf{x}_O)$ in Eqn. 9.

These M samples $\{(\hat{\mathbf{x}}_U, \mathbf{x}_O)\}_{m=1}^M$ are then fed into diagnosis model $f_\phi(\cdot)$, leading to a set of softmax prediction distributions on \mathbf{x}_ϕ , denoted by $\{(p^{(1)}, \dots, p^{(|\phi|)})^m\}_{m=1}^M$. Then, we calculate the expectation $\boldsymbol{\mu}_{f_\phi} = \mathbb{E}[p^{(1)}, \dots, p^{(|\phi|)}]$ and standard deviation $\boldsymbol{\sigma}_{f_\phi} = \sqrt{\text{Var}[p^{(1)}, \dots, p^{(|\phi|)}]}$ of $f_\phi(\cdot)$ as diagnostic bases.

Inspired by Lin et al. [21], FIT would stop inquiring to inform the chosen disease if the probability of the chosen disease is high enough so that inquiring more symptoms would not overturn the diagnosis. That is, inquiry process would stop when the probability of the chosen disease is beyond the upper bound of the 6σ confidence interval [27, 26] of other disease probabilities. Dealing with single chosen disease d , where $d = \text{argmax}_j \boldsymbol{\mu}_{f_\phi}^{(j)}$, the stop criterion can be formulated as:

$$\forall j \neq d, \boldsymbol{\mu}_{f_\phi}^{(d)} > \boldsymbol{\mu}_{f_\phi}^{(j)} + 3\boldsymbol{\sigma}_{f_\phi}^{(j)}. \quad (10)$$

4 Related Work

There is a significant amount of previous work dealing with self-diagnosis. One large family of models applies Bayesian inference and tree-based methods [17, 18, 37, 16], which use entropy functions to pick symptoms based on the theory of information gain. For instance, Nan et al. [24, 25] and Zakim et al. [38] proposed to address the cost of feature acquisition by using decision tree and

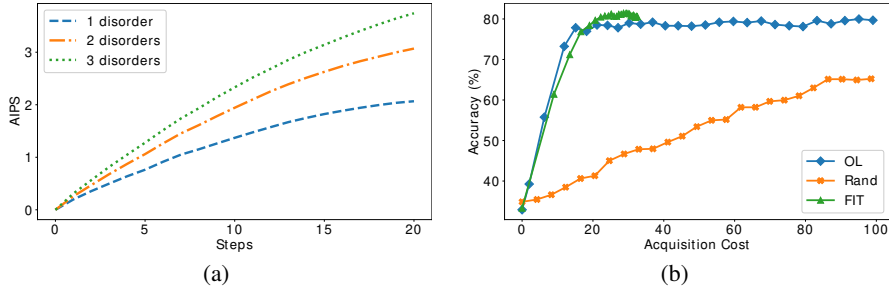


Figure 2: (a) Evolution of AIPS when the number of inquiry steps increases in FIT framework for a multi-disorder setting. (b) Accuracy vs. cost of acquired features of FIT, OL [12] and random method on 1,024 test cases from the diabetes dataset.

random forest methods. In addition to this, Hayashi [8] attempted to extract rule-based representations from medical data and human knowledge to perform disease diagnosis. Early et al. [7], Kachuee et al. [11] suggested sensitivity analysis of trained predictors to measure the importance of each feature given a context. Wang et al. [32] proposed a hierarchical lookup framework based on the symptom embedding where the graph representation learning is tailored towards disease diagnosis. Since global maximization of the information gain or global sensitivity is intractable, these methods often use greedy algorithms or approximation that result in low accuracy.

Recently Janisch et al. [9, 10] show that reinforcement learning (RL) methods outperform tree-based methods in the task of sequential feature acquisition with a given cost function. In particular, Tang et al. [31] first formulated the inquiry and diagnosis process as a Markov decision process and used RL to perform symptom checking based on a simulated environment and data. More recently, Peng et al. [28], Kao et al. [13] achieved competitive results even on medium search spaces. Kachuee et al. [12] proposed a method based on deep Q-learning with variations of model uncertainty as the reward function. Xia et al. [35] used a Generative Adversarial Network (GAN) and policy gradients to implement an RL agent for automatic self-diagnosis. This method shows good performance on two public datasets with Top-1 accuracy equal to 73% and 76.9% for the cases of four and five different diseases, respectively. However, such a low number of diseases is not acceptable.

5 Experiments

We evaluate FIT on two simulated public datasets: SymCAT, a symptom-based disease database [2], and a rare disease database from the Human Phenotype Ontology (<https://hpo.jax.org/app/>), which we utilized initially to test methods on colossal search space. We also report results on two medical dialogue datasets: Dxy [36] and MuZhi [33], a real-world diabetes dataset, and two real rare disease datasets: HMS and MME. All of them are publicly available and without personally identifiable information. Details regarding datasets and model structures are listed in the Appendix. The experiments of FIT below are all implemented with the speedup techniques in Sec. 3.3.

We have selected the most proper and state-of-the-art RL baseline for every dataset. **GAMP** [35] uses GAN to implement an RL agent for symptom checking, which is only proven to be valid on tiny feature space (MuZhi and Dxy datasets). **REFUEL** [28] is a SOTA RL method designed for symptom checking (features are binary). **OL** [12] is based on deep Q-learning, designed for cost-sensitive feature selection. In general, REFUEL is not available for the diabetes dataset because the features are not binary. OL is not optimal for other symptom checking datasets except the diabetes dataset because their feature cost is not defined. However, FIT shows great universality.

5.1 Simulated Datasets

SymCAT Owing to the difficulties in obtaining and sharing medical data under privacy laws (e.g., the Health Insurance Portability and Accountability Act; HIPAA), we follow Kao et al. [13] and work first with simulated medical data. For this, we use the SymCAT symptom-disease database [2], which consists of 801 diseases and 474 symptoms in total. For each disease in SymCAT, there is information about its symptoms including the symptom marginal probabilities. The simulation process first

Table 3: Accuracy of REFUEL [28], GAMP[35] and FIT on two public medical dialogue datasets. The results of FIT are shown in percentage with a 95% confidence interval with 20 random runs.

	REFUEL [28]	GAMP[35]	FIT
MuZhi [33]	71.8	73	72.6 \pm 0.5
Dxy [36]	75.7	76.9	81.1 \pm 0.3

samples a disease and its related symptoms from the set of all diseases. Then, symptoms are generated by performing a Bernoulli trial on each extracted symptom according to its corresponding probability. For instance, if the disease "abscess of nose" is sampled, and the probabilities of "cough" and "fever" under "abscess of nose" are 73% and 62% respectively, we obtain one data instance by sampling Bernoulli random variables according to these probabilities. As in the experiments by Peng et al. [28], we sample 10^6 , 10^5 , and 10^4 data points for training, validation, and testing.

To evaluate the performance of FIT, we follow Peng et al. [28] and form three different disease diagnosis tasks, which contain respectively 200, 300, and 400 diseases to discriminate. The number of possible symptoms is more than 300, while the average number of positive symptoms per patient is about 3. We list more properties of the dataset in the Appendix. Typically, it is tough to identify positive symptoms. Hence, besides predictive accuracy, we also report *the average number of inquired positive symptoms*, which we abbreviate as AIPS. At the beginning of the inquiring process, one positive symptom is chosen uniformly at random among the positive symptoms for that patient, in particular as a patient self-report. So the maximum AIPS is about 2.

In the Appendix we show how accuracy and AIPS change as the number of maximum inquiry steps increases on the test set. M was selected to be 100. According to this, to perform as few steps as possible, we set the number of maximum inquiry steps to 15, 16, and 17 respectively for the tasks with 200, 300, and 400 diseases on 10,000 test patients and report results in Table 2. We choose REFUEL [28] as a baseline and *set the numbers of maximum inquiry steps to the same as FIT*. We can see that FIT outperforms REFUEL in every metric. With the same maximum number of steps, the RL agent would stop earlier and make an inferior prediction, which shows the advantages of FIT's stop criterion. REFUEL believes it has enough evidence to stop and make predictions while FIT proves that wrong, because, with several more queries, FIT could provide a significantly better result, which is of importance, especially in the medical domain. We present comparisons with a commensurate number of queries in the Appendix, which shows FIT still outperforms REFUEL on Top3 and Top5.

Note that we could easily extend FIT to handle co-morbidity, i.e., suffering from multiple diseases. In this case, the different disease variables are considered to be independent. For the extension, all we need to change is to train a multi-label diagnosis model instead of a multi-class one. Since we have not sought out appropriate data, we present a simple experiment in Figure 2(a). In the aforementioned 200-disease task, we generate test datasets of 2 and 3 disorders, which sample 2 and 3 diseases and their related symptoms respectively to perform a Bernoulli trial. We can see that although FIT is just trained with single disorder data, it maintains a quick growth rate of AIPS with multi-disorder data.

Human Phenotype Ontology The Human Phenotype Ontology (HPO) provides a standardized vocabulary of phenotypic abnormalities for human disease. So far, HPO includes over 13,000 terms and 156,000 expert annotations to human hereditary diseases, obtained from multiple sources (the medical literature, Orphanet (<https://www.orpha.net/>), and OMIM (<https://omim.org/>)). We downloaded diseases and related symptoms from the public rare disease dictionary, including 11,441 diseases, 13,032 annotated symptoms, and marginal probabilities. We consider two different tasks, each containing 500 and 1000 diseases to discriminate. Our goal is to evaluate FIT in settings in which **the number of symptoms is higher and closer to real-life applications: the numbers of symptoms are 1,901 and 3,599 respectively, which is six times larger than in SymCAT**. The average numbers of positive symptoms per patient are 6.11 and 9.07. We generated 10,000 patients and set the maximum inquiry steps to 10 and 20 for the tasks with 500 and 1000 diseases, respectively. M was fixed to 20. While training REFUEL, the numbers of maximum inquiry steps are set to 14 and 20, respectively. We show results for FIT and REFUEL in Table 1. In this case, **FIT outperforms REFUEL by a larger magnitude than before** with the accuracy of FIT being at least 10 percent units larger and the number of steps decreasing when compared to REFUEL.

Table 4: Accuracy of REFUEL [28] and FIT on two public rare disease datasets. The results of FIT framework are shown in percentage with a 95% confidence interval with 20 random runs.

DATASET	REFUEL [28]				FIT			
	TOP1	TOP3	TOP5	#STEPS	TOP1	TOP3	TOP5	#STEPS
HMS	18.22	34.07	45.31	11.26	34.22 ± 0.93	61.39 ± 1.12	68.43 ± 1.12	13.40 ± 0.06
MME	48.15	58.40	67.33	9.23	60.70 ± 1.28	79.53 ± 1.40	83.37 ± 0.86	10.14 ± 0.14

5.2 Real-Life Datasets

Medical Dialogue Datasets Wei et al. [33] constructed the MuZhi Medical Dialogue dataset, which uses collected dialogue data from the pediatric department of a Chinese online healthcare website (<https://muzhi.baidu.com/>). MuZhi includes 66 specific symptoms and 4 diagnosed diseases: children’s bronchitis, children’s functional dyspepsia, infantile diarrhea infection, and upper respiratory infection. There are 710 dialogue data points, representing different patients.

The Dxy Dialogue Medical dataset [36] contains data from a prevalent Chinese online healthcare website (<https://dxy.com/>), where people often inquire experts for professional medical advice. This dataset contains 527 dialogue data points, representing different patients, 5 diagnosed diseases, and 41 specific symptoms. Both datasets are already in the form of disease-symptoms pairs.

Table 3 shows results for REFUEL [28], GAMP [35] and FIT on MuZhi and Dxy. We implemented FIT by setting M to 100. The maximum number of inquiry steps are 16 and 20 for MuZhi and Dxy, respectively, which were both set to 20 for GAMP [35] and REFUEL. The results show that FIT has competitive performance on these datasets, with slightly better accuracy than baselines.

Diabetes Dataset Beyond symptom checking, Figure 2(b) shows evaluation on a real-world health dataset for diabetes classification, which was arranged by Kachuee et al. [12] from the national health and nutrition examination survey (NAHNES) [1] data. The final dataset consists of 92,062 instances of 45 features, which contains: demographic information, lab results (total cholesterol, triglyceride, etc.), examination data (weight, height, etc.), and questionnaire answers (smoking, alcohol, etc.). An expert with experience in medical studies suggested costs for each feature based on the overall financial burden, patient privacy, and patient inconvenience. Finally, the fasting glucose values were used to define three classes: normal, pre-diabetes, and diabetes based on standard threshold values. The dataset is randomly split to 15% for test, 15% for validation, and the rest for train. We set M to 200 and maximum inquiry steps were not limited. Note that the speedup techniques in Sec. 3.3 are not available here because they rely on the enormosity and discreteness of features. As it can be observed from Figure 2(b), FIT framework achieves a superior accuracy *with a lower acquisition cost* compared to OL [12], which even leverages acquisition cost during training.

Rare Disease Datasets HMS is collected from [15], which sampled 93 rare disease cases from original real-life health records by exclusion criteria, including lack of confirmed diagnosis, lack of visit information, and main content. Finally, we chose 83 cases containing 747 symptoms and 37 different diagnoses with at least one matched HPO disease term and one matched symptom term.

The Matchmaker Exchange API (<https://github.com/ga4gh/mme-apis/>) provides a shared language that databases can use to query each other to find similar patients. The API is built around a standardized patient profile including both phenotype and genotype information. MME is the standardized test set of Matchmaker Exchange API at rare disease domain, containing 50 de-identified patients selected from publications. We chose 43 patients containing 559 symptoms and 18 different diagnoses with at least one matched HPO disease term and one matched symptom term.

We initially propose to verify the effectiveness of simulated train data on public knowledge bases. Specifically, we train FIT by simulated data based on HPO entries with matched disease codes from HMS and MME. Note that HMS and MME are just test sets. We fixed M to 100 and the number of maximum inquiry steps to 15 for REFUEL [28] and FIT. The results are reported in Table 4. As shown, FIT achieves superior performance, but there can be room for improvement owing to the discrepancy of symptom distributions between the HPO knowledge base and these real-world data.

6 Conclusion

We have proposed FIT, an information-based framework for fast and accurate disease self-diagnosis, which shows better performance than prior methods [31, 28, 22, 35]. We adopt a PoE Encoder to efficiently handle missing data and design a two-step sampling strategy to improve the quality of the generated samples. Both contributions result in higher disease diagnostic accuracy. We slightly modify previous calculations of the information reward to significantly speed up inference to a practical level in real-life settings while maintaining good disease-prediction accuracy. As the experiments show, our results in two simulated datasets, SymCAT and HPO, outperform existing baselines and reveal that FIT can effectively deal with colossal search space problems at a small cost of time. Furthermore, we evaluate FIT on two real-life dialogue datasets and achieve competitive performance. Moreover, besides symptom checking, the results on the diabetes dataset show potential of FIT in diagnosis with more comprehensive features. Besides, we initially verify the effectiveness of simulated train data based on public knowledge with two real-world rare disease datasets.

References

- [1] National health and nutrition examination survey. <https://www.cdc.gov/nchs/nhanes>, 2018.
- [2] AHEAD Research Inc. Symcat: Symptom-based, computer assisted triage. <http://www.symcat.com>, 2017.
- [3] Yanshuai Cao and David J Fleet. Generalized product of experts for automatic and principled fusion of gaussian process predictions. *arXiv preprint arXiv:1410.7827*, 2014.
- [4] Edward Choi, Mohammad Taha Bahadori, Andy Schuetz, Walter F Stewart, and Jimeng Sun. Doctor ai: Predicting clinical events via recurrent neural networks. In *Machine Learning for Healthcare Conference*, pages 301–318, 2016.
- [5] Edward Choi, Mohammad Taha Bahadori, Jimeng Sun, Joshua Kulas, Andy Schuetz, and Walter Stewart. Retain: An interpretable predictive model for healthcare using reverse time attention mechanism. In *Advances in Neural Information Processing Systems*, pages 3504–3512, 2016.
- [6] Edward Choi, Zhen Xu, Yujia Li, Michael Dusenberry, Gerardo Flores, Emily Xue, and Andrew Dai. Learning the graphical structure of electronic health records with graph convolutional transformer. In *Proceedings of the AAAI Conference on Artificial Intelligence*, volume 34, pages 606–613, 2020.
- [7] Kirstin Early, Stephen E Fienberg, and Jennifer Mankoff. Test time feature ordering with focus: Interactive predictions with minimal user burden. In *Proceedings of the 2016 ACM International Joint Conference on Pervasive and Ubiquitous Computing*, pages 992–1003, 2016.
- [8] Yoichi Hayashi. A neural expert system with automated extraction of fuzzy if-then rules and its application to medical diagnosis. In *Advances in neural information processing systems*, pages 578–584, 1991.
- [9] Jaromír Janisch, Tomáš Pevný, and Viliam Lisý. Classification with costly features using deep reinforcement learning. In *Proceedings of the AAAI Conference on Artificial Intelligence*, volume 33, pages 3959–3966, 2019.
- [10] Jaromír Janisch, Tomáš Pevný, and Viliam Lisý. Classification with costly features as a sequential decision-making problem. *Machine Learning*, pages 1–29, 2020.
- [11] Mohammad Kachuee, Sajad Darabi, Babak Moatamed, and Majid Sarrafzadeh. Dynamic feature acquisition using denoising autoencoders. *IEEE transactions on neural networks and learning systems*, 30(8):2252–2262, 2018.
- [12] Mohammad Kachuee, Orpaz Goldstein, Kimmo Kärkkäinen, Sajad Darabi, and Majid Sarrafzadeh. Opportunistic learning: Budgeted cost-sensitive learning from data streams. In *International Conference on Learning Representations*, 2018.

- [13] Hao-Cheng Kao, Kai-Fu Tang, and Edward Y Chang. Context-aware symptom checking for disease diagnosis using hierarchical reinforcement learning. In *Thirty-Second AAAI Conference on Artificial Intelligence*, 2018.
- [14] Diederik P Kingma and Max Welling. Auto-encoding variational bayes. *arXiv preprint arXiv:1312.6114*, 2013.
- [15] Johannes Knitza, Koray Tascilar, Eva-Maria Messner, Marco Meyer, Diana Vossen, Almut Pulla, Philipp Bosch, Julia Kittler, Arnd Kleyer, Philipp Sewerin, et al. German mobile apps in rheumatology: review and analysis using the mobile application rating scale (mars). *JMIR mHealth and uHealth*, 7(8):e14991, 2019.
- [16] Ron Kohavi. Scaling up the accuracy of naive-bayes classifiers: A decision-tree hybrid. In *Kdd*, volume 96, pages 202–207, 1996.
- [17] Igor Kononenko. Inductive and bayesian learning in medical diagnosis. *Applied Artificial Intelligence an International Journal*, 7(4):317–337, 1993.
- [18] Igor Kononenko. Machine learning for medical diagnosis: history, state of the art and perspective. *Artificial Intelligence in medicine*, 23(1):89–109, 2001.
- [19] Robert S Ledley and Lee B Lusted. Reasoning foundations of medical diagnosis. *Science*, 130(3366):9–21, 1959.
- [20] Yoav Lewenberg, Yoram Bachrach, Ulrich Paquet, and Jeffrey S Rosenschein. Knowing what to ask: A bayesian active learning approach to the surveying problem. In *AAAI*, pages 1396–1402, 2017.
- [21] Junfan Lin, Ziliang Chen, Xiaodan Liang, Keze Wang, and Liang Lin. Learning reinforced agents with counterfactual simulation for medical automatic diagnosis. *arXiv preprint arXiv:2003.06534*, 2020.
- [22] C Ma, S Tschitschek, K Palla, JM Hernández-Lobato, S Nowozin, and C Zhang. Eddi: Efficient dynamic discovery of high-value information with partial vae. In *36th International Conference on Machine Learning, ICML 2019*, volume 2019, pages 7483–7504, 2019.
- [23] Fenglong Ma, Radha Chitta, Jing Zhou, Quanzeng You, Tong Sun, and Jing Gao. Dipole: Diagnosis prediction in healthcare via attention-based bidirectional recurrent neural networks. In *Proceedings of the 23rd ACM SIGKDD international conference on knowledge discovery and data mining*, pages 1903–1911, 2017.
- [24] Feng Nan, Joseph Wang, and Venkatesh Saligrama. Feature-budgeted random forest. *arXiv preprint arXiv:1502.05925*, 2015.
- [25] Feng Nan, Joseph Wang, and Venkatesh Saligrama. Pruning random forests for prediction on a budget. In *Advances in neural information processing systems*, pages 2334–2342, 2016.
- [26] Pete S. Pande and Larry Holpp. *What Is Six SIGMA?* McGraw-Hill Professional, 2001.
- [27] Emanuel Parzen. *Modern probability theory and its applications*. John Wiley & Sons, Incorporated, 1960.
- [28] Yu-Shao Peng, Kai-Fu Tang, Hsuan-Tien Lin, and Edward Chang. Refuel: Exploring sparse features in deep reinforcement learning for fast disease diagnosis. In *Advances in neural information processing systems*, pages 7322–7331, 2018.
- [29] Hannah L Semigran, Jeffrey A Linder, Courtney Gidengil, and Ateev Mehrotra. Evaluation of symptom checkers for self diagnosis and triage: audit study. *bmj*, 351:h3480, 2015.
- [30] Hajin Shim, Sung Ju Hwang, and Eunho Yang. Joint active feature acquisition and classification with variable-size set encoding. In *Advances in neural information processing systems*, pages 1368–1378, 2018.

- [31] Kai-Fu Tang, Hao-Cheng Kao, Chun-Nan Chou, and Edward Y Chang. Inquire and diagnose: Neural symptom checking ensemble using deep reinforcement learning. In *NIPS Workshop on Deep Reinforcement Learning*, 2016.
- [32] Zifeng Wang, Rui Wen, Xi Chen, Shilei Cao, Shao-Lun Huang, Buyue Qian, and Yefeng Zheng. Online disease self-diagnosis with inductive heterogeneous graph convolutional networks. *arXiv preprint arXiv:2009.02625*, 2020.
- [33] Zhongyu Wei, Qianlong Liu, Baolin Peng, Huaixiao Tou, Ting Chen, Xuan-Jing Huang, Kam-Fai Wong, and Xiang Dai. Task-oriented dialogue system for automatic diagnosis. In *Proceedings of the 56th Annual Meeting of the Association for Computational Linguistics (Volume 2: Short Papers)*, pages 201–207, 2018.
- [34] Mike Wu and Noah Goodman. Multimodal generative models for scalable weakly-supervised learning. In *Advances in Neural Information Processing Systems*, pages 5575–5585, 2018.
- [35] Yuan Xia, Jingbo Zhou, Zhenhui Shi, Chao Lu, and Haifeng Huang. Generative adversarial regularized mutual information policy gradient framework for automatic diagnosis. In *Proceedings of the AAAI Conference on Artificial Intelligence*, volume 34, pages 1062–1069, 2020.
- [36] Lin Xu, Qixian Zhou, Ke Gong, Xiaodan Liang, Jianheng Tang, and Liang Lin. End-to-end knowledge-routed relational dialogue system for automatic diagnosis. In *Proceedings of the AAAI Conference on Artificial Intelligence*, volume 33, pages 7346–7353, 2019.
- [37] Zhixiang Xu, Matt Kusner, Kilian Weinberger, and Minmin Chen. Cost-sensitive tree of classifiers. In *International conference on machine learning*, pages 133–141, 2013.
- [38] David Zakim, Niko Braun, Peter Fritz, and Mark Dominik Alscher. Underutilization of information and knowledge in everyday medical practice: Evaluation of a computer-based solution. *BMC Medical Informatics and Decision Making*, 8(1):50, 2008.